Proceedings of the 28th IEEE
EMBS Annual International Conference
New York City, USA, Aug 30-Sept 3, 2006

Anatomically Realistic Torso Model For Studying the Relative Decay of Gastric Electrical and Magnetic Fields

L. K. Cheng, M. L. Buist and A. J. Pullan

Abstract— **Non-invasive assessment of the gastro-intestinal system has not obtained widespread clinical acceptance despite the fact that the first electrogastrograms were recorded almost a century ago. One technique that is gaining acceptance for non-invasively assessing the gastrointestinal system is the recording of cutaneous electrogastrograms. It has been proposed that measurement of the gastric magnetic field (magnetogastrogram) may produce more reliable signals in the form of a vector field and also allows the signals to be obtained with non-contact sensors.**

In this study, an anatomically realistic torso model of the gastrointestinal system is used to investigate the relative decay of electrical and magnetic fields resulting from gastric electrical activity. Typically the electrical fields are measured on the skin surface while the magnetic fields are recorded at locations close to, but not in contact with the skin surface. This is the first study which has used a temporal and multiple dipole source model to simulate resultant electrical and magnetic fields.

I. INTRODUCTION

The development of non-invasive methods for assessing gastrointestinal (GI) electrical activity has been unremarkable when compared to the success of the electrocardiogram (ECG). The ECG was first discovered by Waller in 1887 [1] while the electrogastrogram (EGG) was discovered by Alvarez in 1922 [2]. Since those initial discoveries the ECG has now become a routine diagnostic tool while the reliability and usefulness of the EGG is subject to some debate [3], [4].

The electrical activity detectable on the body surface of GI origin is very weak. This is due to the relatively thin muscular components within the walls of the GI tract, attenutation of the signal by the subcutaneous fat and skeletal musculature layers [5], the distance from the source to the recording electrodes, and the masking effects of other biological signals present in the body (predominantly of cardiac and respiratory noise) and most importantly the relatively small signals the source.

Previous simulation studies have shown that magnetic fields are not as affected by low conductivity layers as electrical potentials. However, these studies have been restricted to simplified models of the stomach (*e.g.,* cylinders and cones) [6] and simplified cylindrical representations of the torso [7], [8]. Also of significance is that many of these models have employed simple static dipole sources which are also aligned with global axis of the volume conductor.

L. K. Cheng and A. J. Pullan are with the Bioengineering Institute, The University of Auckland, New Zealand; email (l.cheng@auckland.ac.nz).

M. L. Buist is with the Division of Bioengineering, National University of Singapore

This work was financially suppoprted by a RSNZ (Royal Society of New Zealand) Marsden Grant (UOA320), RSNZ James Cook Fellowship, and the National Institutes of Health (R01 DK64775).

It is believed that the use of non-invasive magnetic field detectors may provide more reliable and possibly additional information not currently available in cutaneous recordings of electrical potentials. The use of a magnetic field recording device also allows the fields to be acquired without direct contact with the subject, thus eliminating the problems associated with skin-electrode contact.

We present here computational simulations of electrical and magnetic fields using an anatomically realistic torso model and a temporally varying multi-dipole source generated from simulated gastric slow wave activity. The electrical and magnetic fields were computed at selected locations within and on the torso volume, and the relative attenuation of each of the fields were compared.

II. METHODS

A. Geometric Model

The geometric model initially described in [9] has been extended to include boundary element representations of the skeletal muscle and subcutaneous fat layers. The model has been constructed from manually digitized axial images from the Visible Human project [10] (as shown in Fig. 1). The digitised points have then be fitted using a least-squares fitting method similar to that presented in [11]. The full geometric model used in the simulations is shown in Fig. 2.

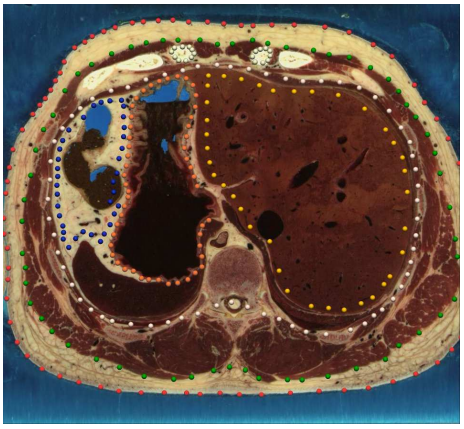

Fig. 1. Digitised axial slice from the Visible Human Project at the mid-sternal level. Digitised on this slice are the stomach (orange points), liver (gold points), small intestine (blue points), muscle, fat (green points), and skin (red points) surfaces.

B. Gastric Sources

Dipole sources with both temporarally varying locations and orientations were used to provide electrical sources

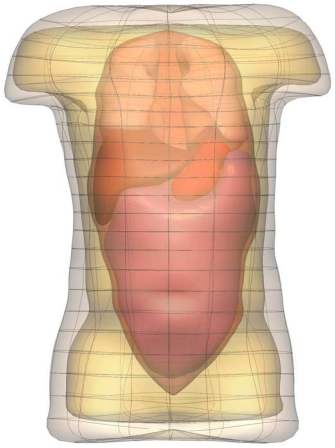

Fig. 2.
Anatomically realistic geometric torso model constructed from data. The model is composed of boundary element representations of the skin, subcutaneous fat, skeltal muscle, intestines, and stomach surfaces. Also shown (but not included in simulations) are the surfaces representing the liver and lung masses.

within the gastric region [12]. These dipole sources were derived from bidomain based simulations of the gastric musculature. From the activation solutions, equivalent dipole sources ($\mathbf{J}$) were calculated based on the local conductivity tensors and transmembrane potential gradients as follows:

$$\mathbf{J} = -\left(\frac{\sigma_i \sigma_e}{\sigma_i + \sigma_e} \nabla V_m\right) \tag{1}$$

where σ_i and σ_e are the intra- and extracellular conductivities and V_m is the transmembrane potential. The electrical activity of the stomach was represented using 320 dipoles (one dipole per geometric element) at 56 discrete time points during a simulated gastric slow wave.

C. Forward Solution

Using the dipole sources described above, resulting potential and magnetic fields were calculated within the torso (and in the case of the magnetic field, external to the body surface). These calculations assumed that the only active sources of electrical activity in the torso originated in the stomach and that all other regions in the torso were electrically passive.

The dipole sources were used to compute electrical potentials on the body surface by solving the Poisson equation,

$$\nabla \cdot (\sigma \nabla \phi) = \nabla \cdot \mathbf{J} \tag{2}$$

where the source term $\mathbf{J}$ is due to the equivalent dipole sources defined in Eqn. 1 and ϕ is the electrical potential field and σ are the conductivities of the tissue.

The potential solution was then used along with the dipole sources to calculate the magnetic field ($\mathbf{B}$) which surrounds the torso by solving Eqn. 3

$$B = \nabla \times A \tag{3}$$

where the vector potential field $\mathbf{A}$ is defined by the electric current density specified in Eqn. 4,.

$$\mathbf{A} = \mu_0 \int_\Omega (J - \sigma \nabla \phi)\, \omega d\Omega \tag{4}$$

where μ_0 is the permeability of free space ($4\pi \times 10^{-7} H/m$).

The different regions of the torso were assigned conductivity values based on simulation studies [13], [8], [14] and experiments [15], [16] as summarized in Tab. I. Note that as our geometric torso is described using boundary elements we have not explicitly included thin membranous surfaces such as the omentum and skin (in contrast to the study presented in [8]). In addition, each region is assumed to electrically homogenous (*e.g.,* as shown by the pink surface in Fig. 2, the cavity region corresponds to the small and large intestine which is modeled as an enclosed region which is electrically isotropic).

Region	Conductivity (mS/mm)
Stomach	0.125
Cavity	0.22
Skeletal Muscle	0.45
Subcutaneous Fat	0.04

TABLE I
BIDOMAIN AND PASSIVE ELECTRICAL CONDUCTIVITIES OF EACH BOUNDARY ELEMENT REGION USED IN THE NUMERICAL SIMULATIONS.

III. RESULTS

The activation profile has been derived from bidomain simulations of the electrical activity in the stomach [17]. Fig. 3(a) shows the dipoles and the activation wave on the stomach surface 8 s after the start of the simulation. Fig. 3(b) shows the corresponding electrical fields on the stomach, muscle, fat and skin surfaces shown as color field (red most positive potential and blue most negative potential).

The magnetic and electric fields were evaluated at locations through the wall of the abdomen as indicated by the white spheres in Fig. 4 and the magnetic and potential field traces plotted in Fig. 5.

Fig. 5(a) shows potential traces from one set of sample locations through the abdomen. The corresponding x, y and z magnetic field intensity components are shown in Fig. 5(b, c and d) where the y coordinate is in the anterior/posterior plane and x is in the saggital plane .

IV. DISCUSSION

We have shown in a simulation study the relative rates of decay of the electrical and magnetic fields which result from the electrical activity of the stomach. The simulation study has allowed us to demonstrate the rates at which the different fields decay through the wall to the abdomen, something which cannot be easily measured in an experimental system.

We have used an anatomically realistic torso model and a complex temporally varying dipole to simulate the magnetic and potential fields. The simulation has shown that the magnetic fields are far more complex than the potential fields which decay monotonically. As the magnetic fields

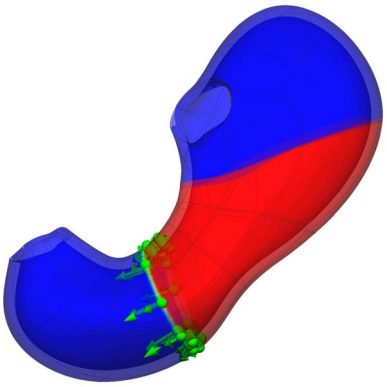

(a) Gastric dipole sources

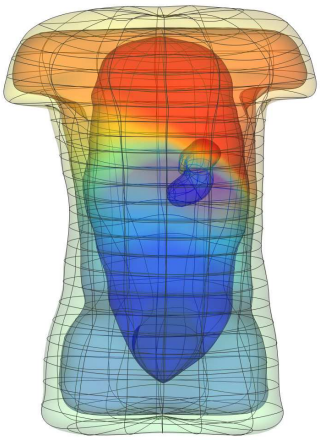

(b) Resultant potential and magnetic fields

Fig. 3. Dipole sources (a) and the corresponding potential fields (b) at 8 s. The dipole sources (green arrows) represent the electrical activity in the stomach musculature. The resulting potential fields on the skin surface are shown as a colored field (red most positive and blue most negative).

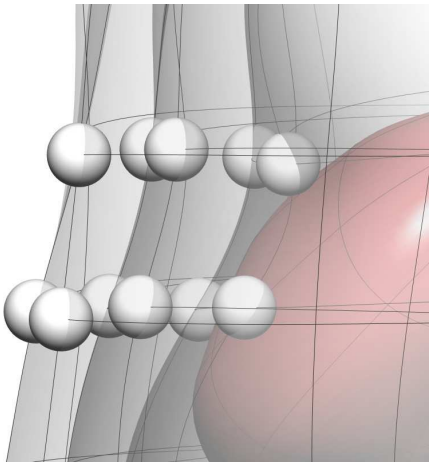

Fig. 4. Locations of the "recording" electrodes (white spheres) on the skin, fat, and muscle surfaces. The magnetic and potential field signals are compared in Fig. 5.

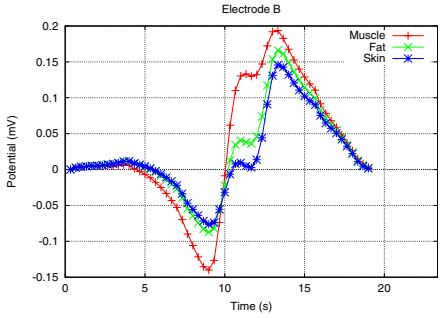

(a) Potential

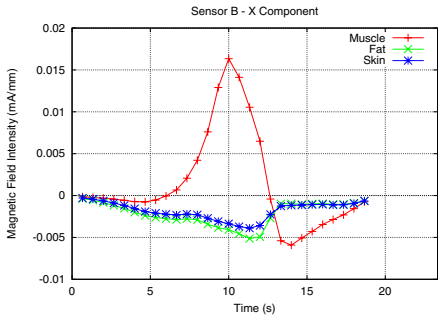

(b) Magnetic Field Intensity X-component

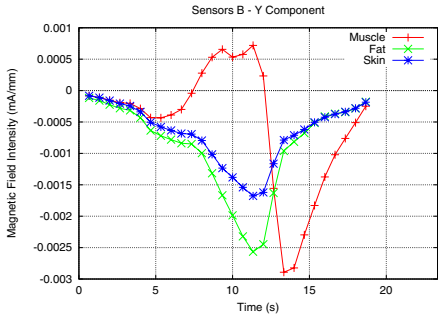

(c) Magnetic Field Intensity Y-component

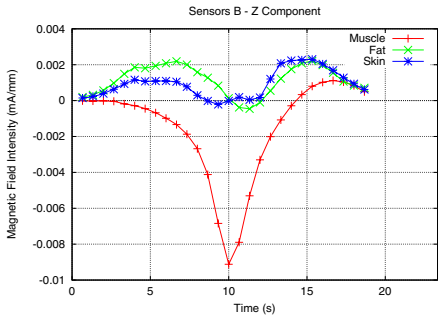

(d) Magnetic Field Intensity Z-component

Fig. 5. Potential traces (a) and corresponding magnetic field intensities at a set of locations located through the abdomen, located above the stomach. Note the fat surface corresponds to the inside surface of the fat layer, and the muscle surface corresponds to the inner surface of the skeletal muscle layer.

are a vector quantity, each component cannot be examined independently. It can be seen in Fig. 5 that while some components decay with distance, due to the vector nature of the magnetic fields, some components may in fact increase in strength. This will require further examination of how the secondary magnetic fields that are generated at the boundaries between regions of different conductivities.

Future studies will also involve investigating "optimal" positions to place the cutaneous electrodes and the magnetic sensors in order to maximize the captured information and reduce signal to noise ratio.

V. ACKNOWLEDGMENT

The authors would like acknowledge the assistance of L. Alan Bradhaw and William O. Richards from Vanderbilt University with this work.

REFERENCES

[1] A. D. Waller, "A demonstration on man of electromotive changes accompanying the heart's beat," *J. Physiol.*, vol. 8, pp. 229–34, 1887.

[2] W. C. Alvarez, "The electrogastrogram and what it shows," *JAMA*, vol. 78, no. 15, pp. 1116–1118, 1922.

[3] M. P. Mintchev, P. Z. Rashev, and K. L. Bowes, "Misinterpretation of human electrogastrograms related to inappropriate data conditioning and acquisition using digital computers.," *Dig Dis Sci*, vol. 45, no. 11, pp. 2137–2144, 2000.

[4] M. L. Buist, L. K. Cheng, K. M. Sanders, and A. J. Pullan, "Multiscale modelling of gastric electrical activity: Can the EGG detect functional electical uncoupling?," *Exp. Physiol.*, vol. 91, pp. 383–390, Jan. 2006. PMID: 16407476.

[5] L. A. Bradshaw, S. H. Allos, J. P. Wikswo Jr, and W. O. Richards, "Correlation and comparison of magnetic and electric detection of small intestinal electric activity," *Am. J. Physiol.*, vol. 272, pp. G1159–G1167, May 1997. PMID: 9176226.

[6] J. Liang and J. D. Chen, "What can be measured from surface electrogastrography. Computer simulations.," *Dig Dis Sci*, vol. 42, no. 7, pp. 1331–1343, 1997.

[7] L. A. Bradshaw, R. S. Wijesinghe, and J. P. Wikswo Jr., "Spatial filter approach for comparison of the forward and inverse problems of electroencephalography and magnetoencephalography.," *Ann. Biomed. Eng.*, vol. 29, no. 3, pp. 214–226, 2001. PMID: 11310783.

[8] L. A. Bradshaw, W. O. Richards, and J. P. Wikswo Jr., "Volume conductor effects on the spatial resolution of magnetic fields and electric potentials from gastrointestinal electrical activity," *Med. Biol. Eng. Comput.*, vol. 39, pp. 35–43, Jan. 2001. PMID: 11214271.

[9] A. J. Pullan, L. K. Cheng, R. Yassi, and M. L. Buist, "Modelling gastrointestinal bioelectric activity," *Prog. Biophys. Mol. Biol.*, vol. 85, pp. 523–550, Jun-Jul 2004. PMID: 15142760.

[10] V. Spitzer, M. J. Ackerman, A. L. Scherzinger, and R. M. Whitlock, "The visible human male: A technical report," *J. Am. Med. Inform. Assoc.*, vol. 3, pp. 118–130, Mar. 1996. PMID: 8653448.

[11] C. P. Bradley, A. J. Pullan, and P. J. Hunter, "Geometric modeling of the human torso using cubic Hermite elements," *Ann. Biomed. Eng.*, vol. 25, pp. 96–111, 1997. PMID: 9124743.

[12] L. K. Cheng, M. L. Buist, R. Yassi, W. O. Richards, L. A. Bradshaw, and A. J. Pullan, "A model of the electrical activity of the stomach: From cell to body surface," in *Proceedings of the 25th Annual International Conference of the IEEE Engineering in Medicine and Biology Society*, (Cancun, Mexico), pp. 2761–2764, Aug. 2003. DOI: 10.1109/IEMBS.2003.1280489.

[13] C. P. Bradley, A. J. Pullan, and P. J. Hunter, "Effects of material properties and geometry on electrocardiographic forward simulations," *Ann. Biomed. Eng.*, vol. 28, no. 7, pp. 721–741, 2000. PMID: 11016411.

[14] P. Czapski, C. Ramon, L. L. Huntsman, G. H. Bardy, and Y. Kim, "Effects of tissue conductivity variations on the cardiac magnetic fields simulated with a realistic heart-torso model," *Phys. Med. Biol.*, vol. 41, no. 8, pp. 1247–1263, 1996. PMID: 8858718.

[15] S. Rush, J. A. Abildskov, and R. McFee, "Resistivity of body tissues at low frequencies," *Circ. Res.*, vol. 12, pp. 40–50, 1963.

[16] L. A. Geddes and L. E. Baker, "The specific resistance of biological material - a compendium of data for the biomedical engineer and physiologist," *Med. & Biol. Engng.*, vol. 5, pp. 271–293, 1967.

[17] L. K. Cheng, J. M. Bodley, and A. J. Pullan, "Comparison of potential and activation based formulations for the inverse problem of electrocardiology," *IEEE Trans. Biomed. Eng.*, vol. 50, pp. 11–22, Jan. 2003.